Available online at www.sciencedirect.com

SCIENCE DIRECT

Cement and Concrete Research 35 (2005) 1797–1803

Cement and Concrete Research

Influence of the migration of chloride ions on the electrochemical impedance spectroscopy of mortar paste

J.M. Loche, A. Ammar*, P. Dumargue

Laboratoire d'Etudes des Phénomènes de Transfert Appliqués au Bâtiment (LEPTAB), Université de La Rochelle, Avenue Michel Crépeau, 17042 La Rochelle cedex-France

Received 26 August 2003; accepted 28 July 2004

Abstract

During the last decade, electrochemical impedance spectroscopy (EIS) started to be effectively exploited to investigate the electrical properties of hydrated cement pastes.

This paper is devoted to the study of the high- and medium-frequency regions of the impedance spectrum and focused on determining the relationship between chloride migration and impedance spectroscopy in accelerated diffusion tests carried out on samples of mortar.

After introducing an experimental protocol based on a four-electrode arrangement, we present the results of a parametric study which is related to the thickness and water–cement ratio (W/C) of the samples.

Firstly, all our measurements show that the presence of chloride ions modifies the impedance response of mortar and reveals a small loop as of modification of the composition of the upstream solution. This loop is probably due to the development of interfacial phenomena between material and the solution.

Secondly, as the migration of chloride process progresses, an increase followed by a decrease of the bulk electrical resistance is observed, whereas the second loop, due to the presence of chlorides, remains constant.

An equivalent electrical circuit is then proposed to fit the different experimental data.

Keywords: Diffusion; Impedance spectroscopy; Migration; Mortar; Transport

1. Introduction

During the last decade, the a.c. impedance technique experienced a promising development in the study of cement-based materials. Indeed, while at the beginning, this non-destructive technique was rather used for the study of electrocristallization mechanisms of the reactions of oxydoreduction and for the electric characterization of the heterogeneous microstructures such as ceramics, the electrochemical impedance spectroscopy (EIS) attracted very quickly a lot of interest and several groups have investigated the electrical response of cement-based systems.

In 1959, Kaesche [1] has published its work related to the application of electrochemical techniques on reinforced concrete using polarization curves to explore whether concrete admixtures may promote steel corrosion. In the 1980s, Andrade et al. [2] investigated the same method to monitor the corrosion rate of steel embedded in carbonated concrete contaminated with chlorides. Several other works followed the same scheme to analyse the evolving microstructure of cement-based materials during hydration, corrosion phenomenon [3–8]. The emphasis of all these contributions was placed on the understanding of the behaviour of cement-based material to different frequencies. Therefore, an electrical model which best fits that behaviour is sought for. More recently, Shi et al. [9] proposed a new method of determination of the diffusion coefficient of

* Corresponding author. Tel.: +33 0546457262; fax: +33 0546458241.
E-mail address: aammar@univ-lr.fr (A. Ammar).

0008-8846/$ - see front matter © 2004 Elsevier Ltd. All rights reserved.
doi:10.1016/j.cemconres.2004.07.040

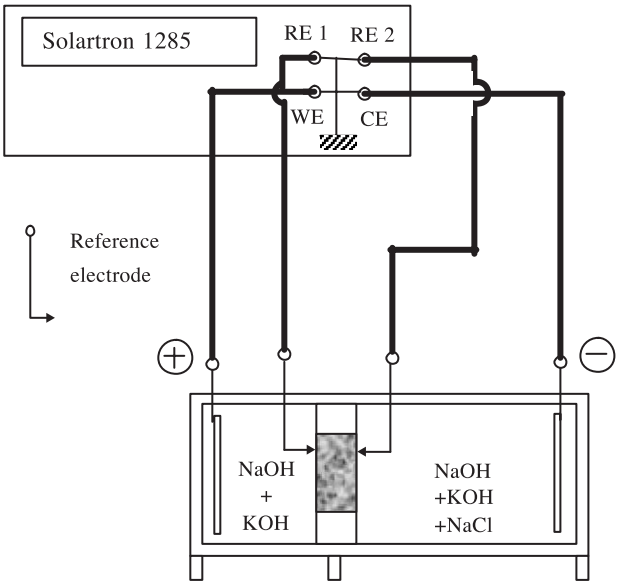

Fig. 1. General diagram of chronoamperometry test. Four-electrode arrangement.

chloride in concrete by using electrochemical impedance spectroscopy.

2. Experimental conditions

2.1. Materials and sample preparation

The mortar samples used in this study were carried out with Portland cement CEM I of class 52.5 MPa and standardized sand whose mass content of silica is higher or equal to 98%. Mortar paste with deionized water was cast in wooden mold of 150×150×180 mm and stored for 48 h at a relative humidity higher than 95%. Afterwards, the specimens were immersed during 90 days in a basic solution containing 1 g/l of NaOH and 4.65 g/l of KOH. Several series of mortar pastes probes were cast for water-to-cement ratios equal to 0.5 and 0.7 and sand-to-cement ratio equal to 1/3.

After curing, a cylindrical sample (diameter=65 mm) has been cored in the central region. Then, slices of different thickness have been sawn. These samples are dried during 7 days at a constant temperature (50 °C) to accelerate drying. The choice of a temperature lower than 70° C have been made to avoid CSH modification by heating as Baroghel-Bouny [10] observed with differential thermic analysis and then saturated with the same basic solution using the method advocated by AFPC-AFREM [11].

All our tests were carried out in a temperature-controlled environment at 21±0.5 °C.

2.2. Electrical measurements and test cells

The chronoamperometry and impedance measurements were performed with the four-electrode arrangement depicted on Fig. 1. In the first step, a constant voltage difference is applied between the two opposite sides of the mortar sample using a Solartron 1285 Electrochemical Interface. This potentiostatic mode uses two platinum electrodes 100 mm in diameter, and two reference electrodes to control the stability of the electrical field through the sample. In a second time, impedance measurements were performed using the Solartron 1260 impedance/Gain-Phase Analyser in voltage drive mode using a logarithmic sweep over the frequency range 50 mHz–10 MHz . Measurement and processing data were supported by Zplot (Scribner associated) software. The reference electrodes used in the chronoamperometry test were then replaced by other electrodes with very low internal impedance. These electrodes were built and tested in our laboratory. Parameters as impedance connexion and induc-

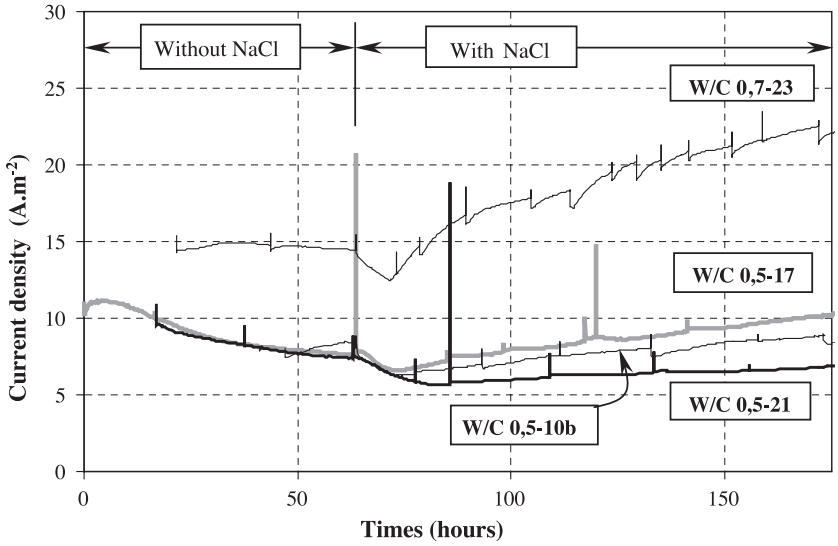

Fig. 2. Chronoamperometry results of four samples: W/C 0.5-10b (W/C=0.5; *L*=10 mm); W/C 0.5-17 (W/C=0.5; *L*=17 mm); W/C 05-21 (W/C=0.5; *L*=21 mm); W/C 0.7-23 (W/C=0.7; *L*=23 mm).

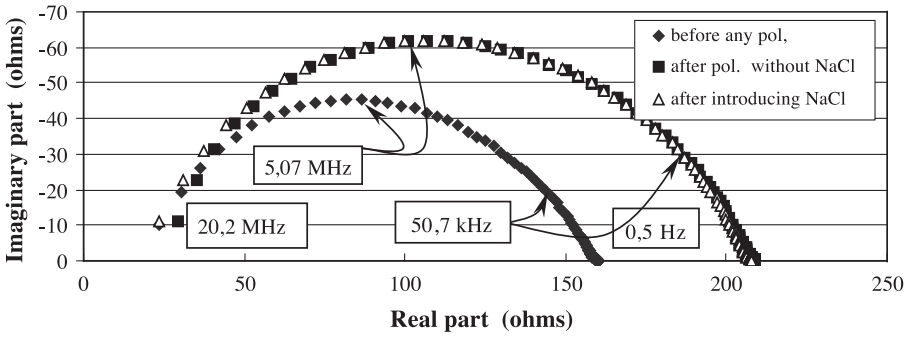

Fig. 3. Nyquist plot data for the W/C=0.5; L=17.4 mm specimen before and after addition of the chloride ions.

tive effects of the leadings were tested. Details about the choice of these electrodes can be found in Ref. [12].

2.3. Main steps of the experiment

Before the impedance measurements, the mortar sample is first polarized and a chronoamperometry is realized based on the scheme shown on Fig. 1. It consists on a current registration in time. This stage takes about 50 h, the necessary time to obtain a stable or slightly increasing current. Fig. 2 exhibits an example of variation of current for different samples. To avoid the Joule effect and the reactions to electrodes, an electrical field of 300 V/m has been adopted for the experimental study. A renewal of the basic electrolyte is undertaken when the stationary current is established and the first impedance measurement is then made. Afterwards, the NaCl with a concentration of 0.5 M is introduced in the upstream of the electrodiffusion cell. Besides, to compute an experimental flux, a chloride dosage was carried out in the downstream of the cell by potentiometric titration with silver nitrate at 0.005 M. The pH and the conductivity have also been measured to ensure the stability of the limit conditions. During the renewal of the downstream solution, we have checked the presence or not of hypochlorite.

3. Experimental results and discussion

It can be seen on Fig. 2 that the current density through the sample decreases when the basic solution with NaCl is added even if this new electrolyte is three times more conductive.

Afterwards, the current density slightly increases whereas the chloride flux remains constant. This is another confirmation of the importance of all species transfer into migration process [13]. The impedance data are plotted in a complex plane known as a Nyquist plot. The first observation that may be drawn is that a measured impedance (Z) of a mortar intersects the Z_r axis at a distance R_0 from the origin (Figs. 3, 4 and 5). Some authors tried to give interpretations to this resistance measured in the high-frequency region. Thus, R_0 has sometimes been defined as a meaningless parameter [7], sometimes attributed to the resistance of the pore solution [3–5]. More recently, Song [14] has explained R_0 as the overall resistance of all the micropores in the concrete bulk, including continuously and discontinuously connected interstitial gel pores, capillary cavities and even microcracks. Our experimentation has shown that the acquisition of impedance measurements beyond 4–5 MHz is a very difficult issue. Over this frequency region, an inductive phenomenon, partly due to coaxial leads, involves significant measurement errors. Besides, nonexperiment has revealed the presence of any circle arc of diameter R_0 to validate the modelization proposed by Song. Therefore, the most convincing interpretation of R_0 remains, in our point of view, the one of Christensen [7].

In the complex graphs given in Figs. 4 and 5, two capacitive branches are clearly identified. The centers of these arcs are located under the real part axis Z_r with a

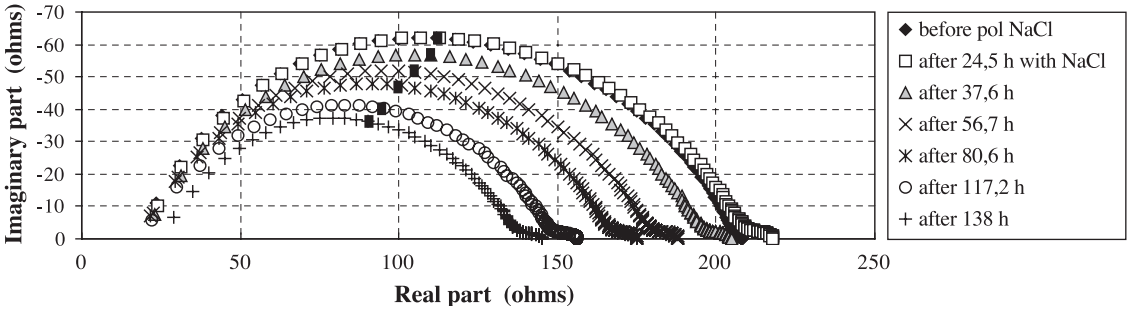

Fig. 4. Evolution of impedance with time for W/C=0.5; L=17.4 mm specimen.

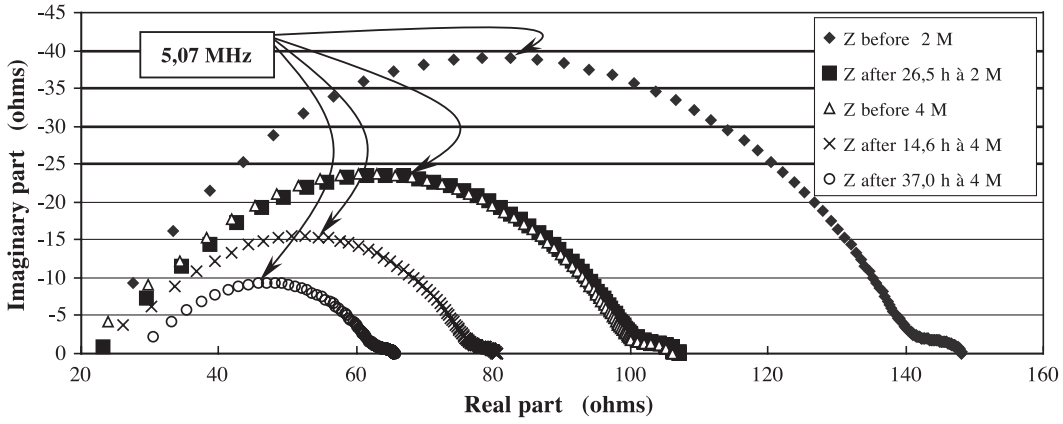

Fig. 5. Evolution of impedance response of mortar sample W/C=0.5; L=17 mm with concentration.

depression angle θ (Fig. 6). We can translate this observation in terms of an equivalent circuit model by a constant phase element (CPE) which is still subject to controversy in the electrochemists' community. The results of the parameter fitting are given in Table 1. The typical features of the EIS Spectra can be summarized by the following:

1) In all cases, the complex graph presents two capacitive loops. The first one, with R_1 as a diameter, is attributed to the whole material composed of a solid phase (continuous and discontinuous paths), a liquid phase and the interface region between these two phases. This interface probably has a significant impact on the electrical behaviour of the material as we will show later. This first arc is defined by the capacitance C_1. Graphs 3 and 4 show the evolution of these two features with respect to the migration time of chloride ions in the mortar paste. We can notice that the adjunction of these ions increases the resistance R_1 which decreases afterwards despite the fact that the flux of chloride ions is constant. However, the capacitance C_1 increases by about 50% of its value when chloride ions are added to the basic solution (NaOH+-KOH) and remains stable as can be seen on Table 1. Its value is closely related to the concentration. Indeed, our experimentation showed that the latter increases by a factor 2 when the concentration moves from 0.5 to 2 M and by a factor 3 when this concentration is set to 4 M (Fig. 5).

2) The second arc is defined by the resistance R_2 and the capacitance C_2. This arc is discernible only when two conditions are satisfied: when the sample is submitted to an electric field and when chlorides are added to the upstream solution. In fact, when impedance measurement is made before polarization, it can be seen that the impedance spectra is not modified by the chloride presence (Fig. 3); this means that the second arc does not correspond to an interfacial capacitive effect between the new chloride solution and the solid section of the sample. As the total migration current measured under the electric field corresponds to the resistance, in this way, the second arc corresponds to an electric effect in the poral conductive solution. When the migration test is achieved, this arc still exists even if chlorides are present into all the length of the pores. In this case, differences in the compositions of the pore solution, upstream and downstream solutions may explain this arc.

If R_2 has the same behaviour as R_1, the capacitance C_2 remains stable. This loop probably reveals an interfacial phenomenon between the sample face and the upstream solution. Tables 2 and 3 show the variation of the electrical features of some samples with respect to the width and to water–cement ratio (W/C), respectively.

3) Very high values for the dielectric constant of mortar paste are obtained (Table 4). Other authors also found increasing values for cement pastes during hydration [7,8]. These high values have been interpreted in terms of

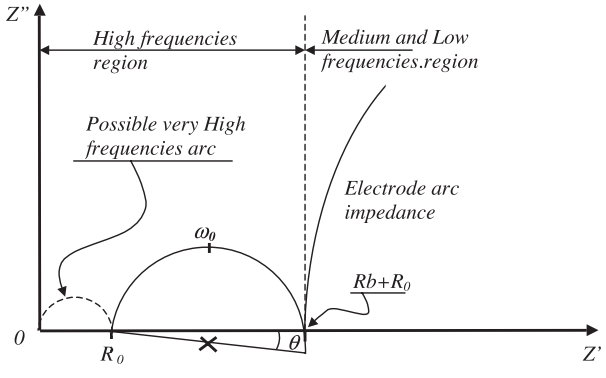

Fig. 6. Complex graph of an R-CPE (Constant Phase Element) circuit in two-point measurement.

Table 1
Results of the parameter fitting

	R_0 (Ω)	R_1 (Ω)	C_1 (10^{-10} F)	n_1	R_2 (Ω)	C_2 (mF)	n_2
Z300A	10.3	103.7	180	0.75	3.6	2.4	0.53
Z300SB	14.0	101.4	246	0.74	21.3	3.2	0.29
Z300SC	14.9	91.5	262	0.74	19.0	3.7	0.29
Z300SF	13.0	86.8	313	0.73	20.8	3.3	0.27

Z300A: before introduction of NaCl; Z300SB: after 12.3 h; Z300SC: after 42 h and Z300SF: after 56 h.

Table 2
Electrical features variation of the mortar samples with thickness

L (mm)	R_0 (Ω)	R_1 (Ω)	C_1 (10^{-10} F)	n_1	R_2 (Ω)	C_2 (mF)	n_2
10.8	13.0	86.8	313	0.730	20.8	3.3	0.27
17.4	15	164	275	0.713	9.9	1.9	0.48
21.3	14	249	150	0.734	41	1.6	0.32

For L=21.3 mm, the exposition time is 70.4 h, whereas for the first and the second sample, it is 56 and 56.8 h, respectively.

Dielectric Amplification Factor (DAF) [7]. Let us emphasize that most of the values reported in the literature are computed by assuming a material to a perfect capacitor (parallel plate capacitor) for which the following formula is applicable [16,17]:

$$C = \frac{\varepsilon_r.\varepsilon_0.A}{d} \tag{1}$$

where A represents the surface area of the plates, d the distance between plates, ε_0 the vacuum permittivity (8.854×10^{-14} F cm^{-1}) and ε_r the relative dielectric constant of the material between plates. Christensen [7] used another formula to compute the dielectric constant. This formula takes into account the fact that the stored response does not correspond to the pure capacitance because the arc center is located under the real axis, as we have previously pointed out.

$$\varepsilon_r = (2\pi\omega_{max})^{\frac{2\theta}{\pi}-1}\frac{d}{R_1 A\varepsilon_0} \tag{2}$$

where θ represents the depression angle given in radians. For a perfect capacitor θ=0; $\omega_{max} = \frac{1}{R_1 C_1}$ is the frequency at the top of the bulk arc or. The other parameters have already been defined.

The values provided by Eqs. (1) and (2) are very different from the expected values of the dielectric constant known for some environments, such as the ceramic (ε_r=100) and air (ε_r=1). Based on this experimental study, we have focused our theoretical research on the solid–electrolyte interfacial region in the pore.

4. Theoretical study

A theoretical analysis of the influence of an external alternating field on the ionic transfer has been carried out [12].

Table 3
Electrical features variation of the mortar samples with W/C

L (mm)	R_0 (Ω)	R_1 (Ω)	C_1 (10^{-10} F)	n_1	R_2 (Ω)	C_2 (mF)	n_2
21.3	14	249	150	0.734	41	1.6	0.32
23.7	27	75	240	0.748	10	8.3	0.33

For L=21.3 mm, the exposition time is 70.4 h, whereas for the second sample, it is 65.7 h.

Table 4
Dielectric constant versus time computed by formulas (1) and (2)

Time (h)	$\varepsilon_{r(1)}$ (10^4)	$\varepsilon_{r(2)}$ (10^5)
0 (without NaCl)	3.10	4.25
63.5 (without NaCl)	1.50	1.30
24.5 (with NaCl; c=0.5 M)	1.61	1.46
37.6 h	1.61	1.45
56.8 h	1.67	1.54
80.6 h	1.55	1.34
117.6 h	1.79	1.68
138 h	1.67	1.42
After 41.5 h without polarization	1.68	1.42
26.5 h (c=2 M)	2.98	2.93
14.6 h (c=4 M)	4.01	3.65
37 h (c=4 M)	5.96	3.70
44 h (c=4 M)	4.62	3.45

All along the pores, the liquid phase is a solution with a high ionic strength; in this way, the double layer Stern model can be resumed as a Helmoltz capacitor and a diffuse layer into the solid material. The equivalent capacity may be calculated from (Eq. (3)):

$$\frac{1}{C_{H\sigma}} = \frac{1}{C_H} + \frac{1}{C_\sigma} \tag{3}$$

where C_H is the Helmoltz layer capacity and C_σ the solid layer capacity. From the ionic average radius of the ions of the basic solution, and knowing the ratio of exchange area ($a_{\sigma L}$:[m^2/m^3]) from Mercury Intrusion Porosimetry, it is possible to roughly evaluate C_H. Assuming the fact in the neutral compact layer, electrostatic pressure is so high that the dielectric constant of water solution is only $\varepsilon^{(L)}=4\varepsilon_0$ [15]. We found $C_H \approx 0.25$ F m^{-2}.

The amplitude of the AC field into the liquid phase may be calculated by the amplitude of the field applied to the solid phase corrected by a dimensionless reducing factor taking into account the influence of the local interfacial charges variations (Eq. (4)). Symbol $_{(+)}$ denotes dimensionless expressions,

$$\tilde{E}_{c0}^{(L)} = \tilde{E}_{c0}^{(\sigma)} + \frac{1}{C_{H\sigma}}\frac{d\tilde{q}_{\sigma 0}}{dx} = \left(1 - E_{Ap+}^{(L)}\right)\tilde{E}_{c0}^{(\sigma)} \tag{4}$$

with $\tilde{E}_{c0}^{(\sigma)} = -\frac{d\tilde{\psi}_{c0}^{(\sigma)}}{dx}$ electric AC field applied to the sample (V/m).

The dimensionless conservation equation of the electric charge may be written (Eq. (5)):

$$\frac{dI_0^{(L)}}{dx_+} = jwa_{\sigma L}\, L\, \tilde{q}_{\sigma 0} \tag{5}$$

with AC current given by Eq. (6):

$$\tilde{I}_0^{(L)} = \varepsilon_L \gamma_{ct}^{(L)} \sigma_B^{(L)}\left[\bar{\Sigma}_+^{(L)}\tilde{E}_{c0}^{(L)} + \bar{A}_{E+}\frac{\tilde{q}_{\sigma 0}}{LC_{H\sigma}}\right] \tag{6}$$

where ε_L, $\gamma_{ct}^{(L)}$ are the open pore porosity and the constrictivity which can be obtained by measuring current through a sample saturated with a known conductivity solution. $\sigma_B^{(L)}$ is the conductivity of this basic solution

without chlorides, $\bar{\Sigma}_{+}^{(L)}$ is a correcting conductivity factor with a value of 1 with basic solution or 4.4 with Ref. [12]. In the bulk material, for frequencies ranging between 2 kHz and 4 MHz, solution of Eqs. (5) and (6) can be found by a development in a power series of $(a_{\sigma L}L)^{-1}$ of $\tilde{E}$sub 0 and $\tilde{q}_{\sigma 0}$. The solution of Eqs. (5) and (6) is given below (Eq. (7)):

$$\tilde{I}_0^{(L)} = \frac{\Delta\tilde{\psi}_{m0}}{(1-\varepsilon_L)\gamma_E^{(\sigma)} + \varepsilon_L\gamma_{ct}^{(L)}} \times \left[\varepsilon_L\gamma_{ct}^{(L)}\bar{\sigma}_B^{(L)} \frac{\bar{\Sigma}_{+}^{(L)}E_{\mathrm{Ap}+} + \bar{A}_{E+}\left(1-\tilde{E}_{Ap+}^{(L)}\right)}{L} + j\omega \frac{C_{H\sigma}\left\{\bar{\Sigma}_{+}^{(L)}\tilde{E}_{\mathrm{Ap}+}^{(L)} + \bar{A}_{E+}\left(1-\tilde{E}_{Ap+}^{(L)}\right)\right.}{\bar{A}_{E+}a_{\sigma L}L} \right] \quad (7)$$

This corresponds to an equivalent parallel circuit RC with:

$$\bar{C}_1 = \frac{C_{\mathrm{H}\sigma}\left\{\bar{\Sigma}_{+}^{(L)}\tilde{E}_{\mathrm{Ap}+}^{(L)} + \bar{A}_{E+}\left(1-\tilde{E}_{\mathrm{Ap}+}^{(L)}\right)\right\}}{\bar{A}_{E+}a_{\sigma L}\left[(1-\varepsilon_L)\gamma_E^{(\sigma)} + \varepsilon_L\gamma_{ct}^{(L)}\right]} \quad (8)$$

and

$$\bar{R} = \frac{\left[(1-\varepsilon_L)\gamma_E^{(\sigma)} + \varepsilon_L\gamma_{ct}^{(L)}\right]L}{\varepsilon_L\gamma_{ct}^{(L)}\sigma_B^{(L)}\left[\bar{\Sigma}_{+}^{(L)}\tilde{\Sigma}_{\mathrm{Ap}+}^{(L)} + \bar{A}_{E+}\left(1-\tilde{E}_{\mathrm{Ap}+}^{(L)}\right)\right]} \quad (9)$$

In these formulas, $\bar{C}_1$ and $\bar{R}_1$ are expressed in F m^2 and Ω m^2, respectively; $\bar{\Sigma}_{+}^{(L)}$ is a corrective parameter of the conductivity. It depends on the adsorption–desorption mechanisms; $\gamma_E^{(\sigma)}$ is a coefficient related to the distortion of the electrical field lines in the solid phase; $a_{\sigma L}$ defines the exchange surface rate between the solid and the liquid phases. This parameter can be determined from a classical mercury porosimetry test; $\tilde{E}_{\mathrm{Ap}+}$ is another parameter related to the applied alternating electrical field. It integrates the induced field from the adsorbed charge distribution at the solid–electrolyte interface; $\bar{A}_{E+}$ is a coefficient defined from the distribution of adsorbed charges, the exchange surface rate $a_{\sigma L}$ and the electrical capacitance ratio of the compact layer and the diffuse layer.

The impedancial response of the material depends on the frequency range. Our experimental results allow us to consider mainly two frequency domains:

* 2 kHz<f<5 MHz: for which a large impedance arc is obtained. It is attributed to the bulk material and can be easily represented by the equivalent circuit R_1C_1, where RC elements are in parallel arrangement (see Fig. 7).
* 5 Hz<f<2 kHz: for which a little loop is obtained. It translates anodic and cathodic interfacial phenomena. Another R_2C_2 equivalent circuit can be used to translate this behaviour. The overall network is a series arrangement. Here, C stands for a constant phase element with both a capacitance component and an arc depression factor. The agreement between our experimental and theoretical results is very satisfactory for $\varepsilon_r \approx 6\varepsilon_0$.

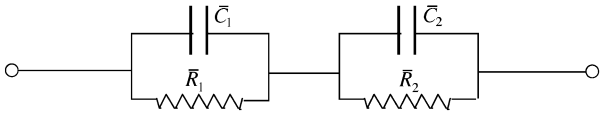

Fig. 7. Detailed equivalent circuit for mortar submitted to electrodiffusion chloride ions.

5. Conclusion

In this work, we have shown that the impedance measurement is a powerful technique for analysing the behaviour of the electrical features of a mortar submitted to the migration of aggressive chloride ions. The main results we have achieved are as follows:

(1) For the high-frequency region, and during the migration of the chloride ions, the electrical resistance of the material decreases according to time whereas the electrical capacitance remains roughly constant for a given concentration.
(2) The addition of chloride ions causes an emergence of the second loop in the complex impedance plane at low frequencies. It might be due to interface phenomena at the entrance of the pores.
(3) The undertaken theoretical study was aimed at showing the significant role of the electrical double layer within the material. This analysis demonstrated that the simplistic modelization of a cement-based material by a plane condenser is not founded. Indeed, the electrical capacity of the material is rather governed by the exchange surface rate between the solid phase and the electrolyte inside pores and not by the section of the tested sample. This explains the very high values of the permittivity suggested by certain authors.
(4) Once again, this technique is efficient, because, coupled with chronoamperometry and the mercury porosimetry, it allows access to some features of the material microstructure.

References

[1] H. Kaesche, Standard test method for half-cell potentials of uncoated reinforcing steel in concrete, Zem.-Kalk-Gips 12 (1959) 289.
[2] C. Andrade, C. Alonso, J.A. Gonzalez, Results of polarization resistance and impedance of steel bars embedded in carbonated concrete contaminated with chlorides, Mat. Sci. Forum 44 and 45 (1989) 329–336.
[3] P. Gu, P. Xie, J.J. Beaudoin, R. Brousseau, AC impedance spectroscopy: (I) a new equivalent circuit model for hydrated portland cement paste, Cem. Concr. Res. 22 (5) (1992) 833–840.

[4] P. Gu, Z. Xu, J.J. Beaudoin, Application of AC impedance techniques in studies of porous cementitious materials: (I) influence of solid phase and pore solution on high frequency resistance, Cem. Concr. Res. 23 (3) (1993) 531–540.
[5] P. Gu, P. Xie, J.J. Beaudoin, R. Brousseau, AC impedance spectroscopy: (II) microstructural characterization of hydrating cement–silica fume systems, Cem. Concr. Res. 23 (1) (1993) 157–168.
[6] P. Xie, P. Gu, Z. Xu, J.J. Beaudoin, A rationalized A.C. impedance model for microstructural characterization of hydrating cement systems, Cem. Concr. Res. 23 (2) (1993) 359–367.
[7] B.J. Christensen, Microstructure studies of hydrating portland cement based materials using impedance spectroscopy, PhD thesis, North Western University, Evanston, Illinois, USA, December 1993.
[8] S.J. Ford, J.H. Hwang, J.D. Shane, R.A. Olson, G.M. Moss, H.M. Jennings, T.O. Mason, Dielectric amplification in cement paste, Adv. Cem. Based Mater. 5 (1997) 418.
[9] Meilun Shi, Zhiyuan Chen, Jian Sun, Determination of diffusivity in concrete by AC impedance spectroscopy, Cem. Concr. Res. 29 (1999) 1111–1115.
[10] V. Baroghel-Bouny, Laboratoire Central des Ponts et Chaussées (Ed.), Caractérisation des pâtes de ciment et des bétons, 1994, pp. 169–170.
[11] AFPC- AFREM, Compte rendu des journées techniques du 11 et 12 décembre 1997, Durabilité des bétons—Méthodes recommandées pour la mesure des grandeurs associées à la durabilité, Laboratoire Matériaux et Durabilité des Constructions, INSA de Toulouse, 165–167.
[12] J.M. Loche, Etude du transfert d'ions chlorures à travers de mortiers de ciment par diffusion–migration. Suivi par spectroscopie d'impédance électrochimique, PhD thesis, University of La Rochelle, France, 2002, 257p.
[13] O. Truc, J.-P. Ollivier, L.-O. Nilsson, Numerical simulation of multi-species transport through saturated concrete during a migration test—MsDiff code, Cem. Concr. Res. 30 (1) (2000) 1581–1592.
[14] G. Song, Equivalent circuit model for AC electrochemical impedance spectroscopy of concrete, Cem. Concr. Res. 30 (11) (2000) 1723–1730.
[15] P. Dumargue, Etude de l'action d'un écoulement liquide turbulent sur la couche double électrique d'une électrode métallique. Application à la mesure des fluctuations de vitesse et de pression en hydrodynamique, State thesis, University of Poitiers, France, 1970.
[16] M. Keddam, H. Takenouti, X.R. Nóvoa, C. Andrade, C. Alonso, Impedance measurements on cement paste, Cem. Concr. Res. 27 (8) (1997) 1191–1201.
[17] C. Andrade, V.M. Blanco, A. Collazo, M. Keddam, X.R. Nóvoa, H. Takenouti, Cement paste hardening process studied by impedance spectroscopy, Electrochem. Acta 44 (1999) 4313–4318.